International Journal of Thin Films Science and Technology

http://dx.doi.org/10.18576/ijtfst/120205

Green Synthesis of Niobium doped Calcium Magnesium Silicate Phosphor Using *Stenotaphrum Secundatum* Grass Extract

Solomon H. Didu, Menberu M. Woldemariam and Nebiyu G. Debelo[*]

Physics Department, College of Natural Sciences, Jimma University, Ethiopia

Received: 21 Feb. 2023, Revised: 22 Mar. 2023, Accepted: 24 Mar. 2023.
Published online: 1 May 2023.

Abstract: Calcium magnesium silicate was synthesized via sol-gel route using calcium carbonate ($CaCo_3$), magnesium carbonate ($MgCo_3$) and *Stenotaphrum secundatum* grass extract (in place of tetraethylorthosilicate - TEOS) as a starting materials. The x-ray diffraction (XRD), Fourier Transform Infra-Red Spectroscopy (FTIR), UV Visible (UV-Vis), Photoluminescence's (PLs) as well as scanning electron microscopy (SEM) and energy dispersive x-ray spectroscopy (EDX) were used to study the phase composition, functional groups identification, absorption spectra determination, examining excitation and emission spectra, surface morphology /microstructure and elemental composition analysis or mapping of the calcined product. The XRD analysis shows that the synthesized samples have tetragonal Calcium Magnesium Silicate - akermanite structure. FTIR confirmed the existence of the functional groups by (Si-O-Si, Si-O, O-Ca-O, O-Mg-O, SiO_4, Ca^{2+}, Mg^{2+}) symmetric stretch, asymmetric stretch, vibrational mode and bending mode in the synthesized samples. UV-Vis revealed the occurrences of maximum absorption at wavelength of 280 nm and it increases in intensity with increasing its Nb^{5+} concentration. PL also shows maximum emission at excitation wavelength of 280 nm at wavelength of 564 nm with emission intensity of 866 a.u. for concentration of 1.0 % Nb^{5+}. In PL analysis, we observe the intensity of emission increasing with increasing concentration of Nb^{5+}**.** SEM images shows that surface microstructures have porous, flux structures and EDX analysis confirmed the presence of all the constituent elements.

Keywords: Akermanite, Nb^{5+} dopant, Green synthesis, TEOS, Luminescent properties.

1 Introduction

Currently, inorganic phosphor materials have drawn out a lot of attention because of their multiple applications, for instance, in cathode-ray tubes, photodiodes, lamps, and x-ray detectors, bio-detectors, color display, radiation dosimetry and dye removal [1-5]. Among the inorganic phosphor materials, silicate based became a lot of attention drawn materials for wide and multi-dimensional practical applications due to their unique features such as visible light transparency, good chemical resistance, high temperature strength, low thermal expansion, excellent conductivity, well known chemical and thermal stability, low cost and easy preparation [6, 7].

Calcium magnesium silicate (CMS) phosphor, with chemical formula $Ca_2MgSi_2O_7$, has recently drawn too much interest due to its unique structure features with an extraordinary physical and chemical stability. It has been also extensively discussed in biological and medical areas of application[2]. Silicate with akermanite structure is becoming a possible and attractive bio-ceramics for tissue engineering applications [3,8]. For instance akermanite calcium magnesium silicate has an extraordinary biocompatibity and excellent bioactivity properties. By now it is becoming a promising bio-ceramic bone tissue engineering materials in medical applications or a probable bone material [6, 9].

In the synthesis of silicate based phosphor materials, tetraethyl-orthosilicate (TEOS) is a primary precursor. Due to its high scarcity in most developing countries and difficulty to import it as well make the challenge magnified. This has been also a bottleneck for the growth of researches focusing on silicate based inorganic phosphor materials in such countries. Therefore, a new mechanism should be designed to alleviate this problem [10, 11]. *Stenotaphrum secundatum* grass is reported to be reach in silica [12] and it is widely available in almost all countries in the world. However, whether the extract of this grass can be used as a precursor for the synthesis of silicate based inorganic phosphors instead of TEOS is not really examined. The use of *Stenotaphrum secundatum* grass extract instead of TEOS has a double advantage in that it is also environmentally friendly.

In our present work, we reported the synthesis and

[*]Corresponding author E-mail: nafsif@gmail.com

characterization of niobium ion doped calcium magnesium silicate phosphor prepared via sol-gel methods. The structural analysis, optical properties, surface morphology and elemental mapping were studied by characterization of x-ray diffractometer, UV-Visible spectrometer, photoluminescence fluorescence spectrophotometer, scanning electron microscope and energy dispersive x-ray spectroscopy analysis, respectively. The different symmetric and asymmetric stretching and vibrational and bending peaks modes were analyzed using Fourier transform infrared spectroscopy.

2 Experimental Sections

2.1 Synthesis

Stenotaphrum secundatum grass was obtained and chopped in to pieces. The grass sample was dried for about one month. The dried sample was then converted to fine powder by grinding mortar and pestle which was precleared with deionized water and ethanol. The fine powder was then added to ten ml of de-ionized water and maintained under magnetic stirring for 30 minutes. Finally the solution was filtered using filter paper and the final *stenotaphrum secundatum* grass extract was stored. Niobium doped Calcium magnesium silicate ($Ca_2MgSi_2O_7$:xNb^{5+}) was then synthesized via sol-gel route using calcium carbonate ($CaCo_3$), Magnesium carbonate ($MgCo_3$) and *Stenotaphrum secundatum* grass extract as a starting materials according to their stoichiometric ratio for various amounts of x (x = 0.2, 0.4, 0.6 and 1.0 % Nb^{5+}) Some amount of the powder samples (0.2, 1.0 % Nb^{5+}) were grinded thoroughly for 2 hrs. using C155 mortar and pestle (Diameter 100 mm, TNB 6EL, England) and the other kept as bulk sample for comparison. The milled sample was put in an alumina crucible and subsequently fired at 500 ^{0}C for one hour. Finally, pure white powder was obtained after cooling down the programmable furnace.

The chemical reaction of the process is given as follows:

$$8CaCO_3 + 4MgCO_3 + 8SiO_2{*}H_2O + 2Nb_2O_5 \rightarrow 4Ca_{(2-x)}MgNbxSi_2O_7 + 12CO_2 (\uparrow) + 8H_2O (\uparrow) + 5\,O_2 (\uparrow) \quad \textbf{(1)}$$

2.2. Characterization

The XRD pattern has been obtained from DRAWELL (XRD-7000 Model: x-ray powder diffractometer using Cu-Kα radiation (λ = 1.5406 Å) at 30 KV, 25 mA and the data were collected over the range of (2Θ = 10 to 80^0). FTIR spectra were recorded with the help of Agilent Technologies: Agilent\MicronLa FTIR transmittance a2m Spectroscopy for examining the functional group (4000 to 400 cm^{-1}) of phosphor by direct use of as- prepared powder sample. The emission and excitation spectra of the samples were measured by Cary Eclipse serial number My1849002 model fluorescence spectrophotometer with slits of emission and excitation lights of 10 nm and 600 nm per minute scanning rates. SEM/EDX (OXFORD INSTRUMENTS; The Business of Science) model was used to identify the surface morphology and examine the elemental mapping and composition of the prepared $Ca_2MgSi_2O_7$:Nb^{5+} phosphor and UV-Vis (the powder was made to solution using di-methyl-sulfoxide (DMSO) solvent keeping the standard proportion of 85:15 solutes to solvent ratio and centrifuge) was used for UV-Vis spectroscopy analysis.

3 Results and Discussion

3.1 XRD Analysis

To identify the phase structure, powder XRD analysis has been carried out. The typical XRD patterns of our sample phosphors were shown in Figure 1. (a, b, c ,d). The XRD pattern of the diffraction peaks of the synthesized samples $Ca_2MgSi_2O_7$:xNb^{5+} Phosphors were matched to the reported results and it was consistent with the standard XRD pattern reported by joint committee on powder diffraction standard (JCPDS) No 77-1149 [13] and (COD card No. 96-900-6941) [14].

Fig.1: (c, d) were zooming image of **(a, b)** patterns respectively to show exact position and shifts of the phosphors for different Nb^{+5} dopants concentrations. Furthermore we observed the effects of dopants in the bulk and milled samples. The XRD pattern analysis shows that the position of peaks slightly shifts to a higher degree position (2Θ= 29.355 to 29.869 ^{0}) as the concentration of dopant, increase from 0.2% to 0.4%. However, no such slight shift was observed for the dopant concentration between 0.4% and 1.0 %. This indicates that the effect of dopants concentration is dominant at low concentration of the dopants. The summary of the first top 3 positions of peaks and intensities is given in **Table .1.**

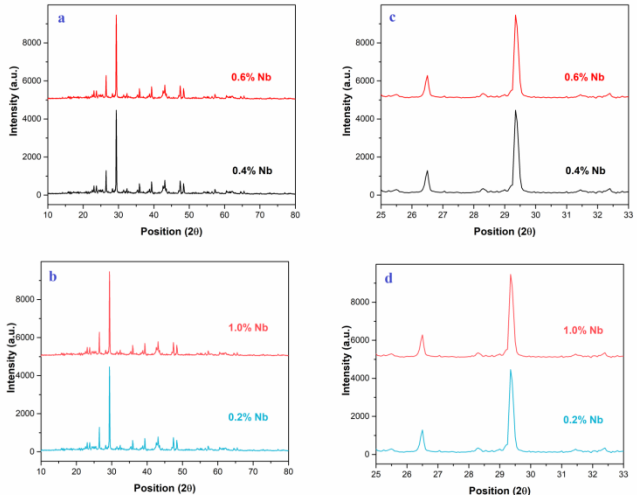

Fig.1: XRD pattern of Niobium doped Calcium Magnesium Silicate Phosphors: bulk (a, c), and milled (b, d).

Using Debye Scherer formula for prominent peak at (211), the average crystallite size (D) of the $Ca_2MgSi_2O_7$:xNb^{5+} phosphor was calculated as **(186) nm**. The formula is represented as follows:

$$D = \frac{k\lambda}{\beta cos\theta} \quad (2)$$

Where, k is the Debye-Scherer constant having value 0.94, λ is wavelength of the incident x-ray (λ=1.5406 Å), β = FWHM (Full Width Half Maximum) of the peaks and Θ corresponding to Braggs diffraction angle.

Table: 1. XRD pattern of top 3 Peaks position (2Θ) and intensities with different dopant (Nb^{5+}) concentration of Calcium Magnesium silicate Phosphor.

Sno	Concentration of Nb^{5+} (%)	Position in (2Θ) in (^{0})	Intensity (a.u.)	Type
1	0.2	29.65	4859	Milled
		26.80	1289	
		43.10	785	
	1.0	29.35	4464	Milled
		26.50	1288	
		43.40	918	
2	0.4	29.80	3354	Bulk
		26.90	1137	
		47.90	683	
	0.6	29.70	3673	Bulk
		26.80	911	
		47.70	653	

XRD pattern **(Fig 1. a, b)** of the powder calcined at a temperature of 500 ^{0}C confirms also the existence of akermanite ($Ca_2MgSi_2O_7$) as the main phase, and merwinite ($Ca_3MgSi_2O_8$) and diopside ($Ca_2MgSi_2O_6$) as the secondary phases. With the increment of the calcination temperature the diopside phase completely disappeared and the intensity of the merwinite peaks reduced gradually. Finally it exists in tetragonal crystal system [14].

As shown in Figure 1. (a, b) and Table 1. For the bulk samples as concentration of dopant (Nb^{+5}) increases from 0.4% at peak position of 29.80 ^{0} to 0.6% at 29.70 ^{0}, the intensity increases from 3354 to 3673 (a.u.). But for the milled one when the concentration of dopant vary from (0.2%) at 29.65 ^{0} to (1.0%) at 29.35 ^{0}, the intensity decreases from 4859 (a.u) to 4464 (a.u). Therefore from our findings, there is significant effect of dopant concentration on the bulk and milled size samples.

3.2 Scanning electron microscope (SEM)

We used SEM to examine the morphology of samples, since the luminescence characteristics of phosphor particles depend on the morphology of the particles such as size, shape, size distribution, and defects so on. The scanning of SEM was performed in the ranges of 1 to 10 micrometer dimension and 1000 to 10,000 times magnifications to see all aspects that demonstrate the morphology of $Ca_2MgSi_2O_7$:xNb^{5+} phosphor. (**See Figure 2. (a = 0.4, b = 0.6 % Nb^{5+} – bulk and C =0.2, d=1.0 % Nb^{5+} - milled)**. From the SEM image result, it was observed that the surface morphology of the particles distributions was not uniform and they were aggregated tightly with each other. Again from the SEM image, it was observed that as prepared samples consists of particles with different size distribution. For milled samples we found relatively uniform distribution of particles on the surface in comparison to bulk (see **Fig. 2**.). It also clearly observed that the surface is rough with different size and shape. At micro level the particles do not separated rather they are in mixed solid solution. Besides it was observed that, there were some large aggregates; it was present as a result of high temperature heat treatment.

SEM images at low magnification (See **Fig. 2**) clearly show significant high magnitude porosity in the bulk powder samples as compared to the grinded ones. When the magnifications become higher, the samples seem to have dense and flux microstructure surface morphology, but still having porosity with different relative density.

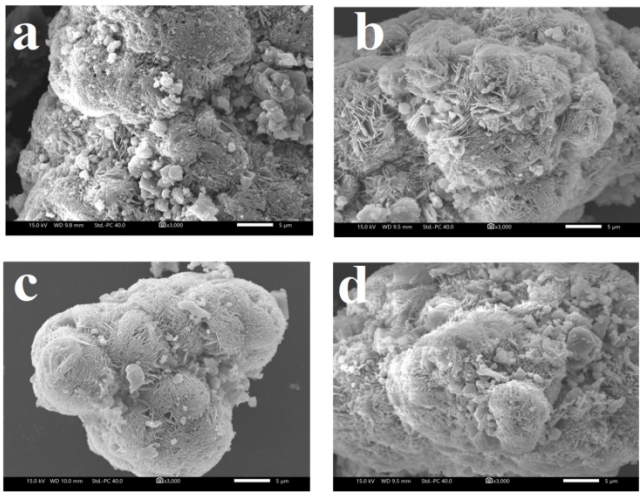

Fig.2: SEM Image of Niobium doped Calcium magnisium Silicate Phosphor : (a=0.4, b=0.6 % Nb – bulk and C =0.2, d=1.0 % Nb - milled).

3.3. Energy dispersive x-ray spectroscopy (EDX)

3.3.1 Energy dispersive x-ray spectroscopy (EDX): Bulk CMS

The elemental composition and mapping of the powder samples were measured using energy dispersive x-ray spectroscopy (EDX). Since EDX spectroscopy is complementary and a standard procedures for determining and quantifying elemental composition of sample area as small as a few nanometers to micrometers, we used it to identify all constitute elements of the as-prepared samples.

The existence of niobium (Nb^{5+}) ion in the corresponding EDX mapping was clearly observed. As expected apart from calcium (Ca), Magnesium (Mg), silicon (Si), niobium (Nb) and oxygen (O) in $Ca_2MgSi_2O_7$:xNb^{5+}, there was no other emission observed in the EDX mapping of the phosphor (see Fig.4). The existence of Ca, Mg, Si, O and Nb, intense peaks are present which preliminarily indicates the formation of $Ca_2MgSi_2O_7$:xNb^{5+} phosphor as shown in (Fig.3).

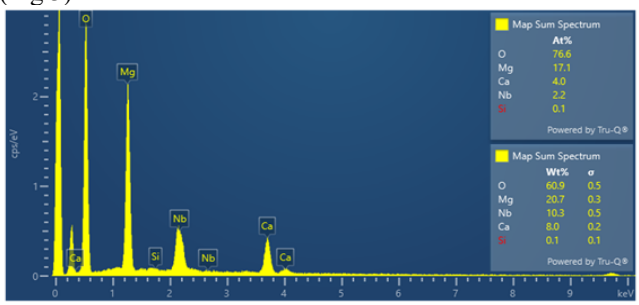

Fig.3: EDX Spectra peaks of Niobium doped Calcium magnisium Silicate phosphor (Bulk).

The EDX Layered image confirms that all the components (calcium, magnesium, silicate, oxygen and dopant niobium) of the CMS are available in the phosphor. For the bulk system the EDX image shows the elemental compositions maps containing Ca, Mg, O, Si and Nb with different amount and proportion as expected. But very small amount of Si is found in the milled CMS, since it was used as catalyst for the solid state reaction in order to avoid sticking of particles with the container walls.

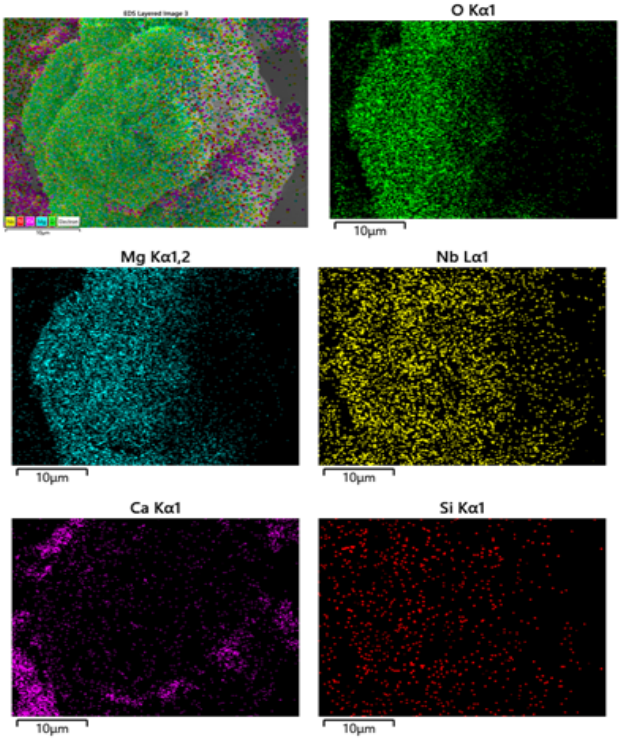

Fig. 4: EDX Maping of Niobium doped Calcium magnisium Silicate phosphor (Map sum Specrum)

3.3.2. Energy dispersive x-ray spectroscopy (EDX): Milled CMS

For milled sample of Niobium doped Calcium Magnesium silicate phosphor, the silica components reduced and different composition in comparison to bulk was observed from the EDX layered images as expected since silica was used as catalyst for the reaction. The sum spectrum of the image shows different percentage amounts and weights of the elements.

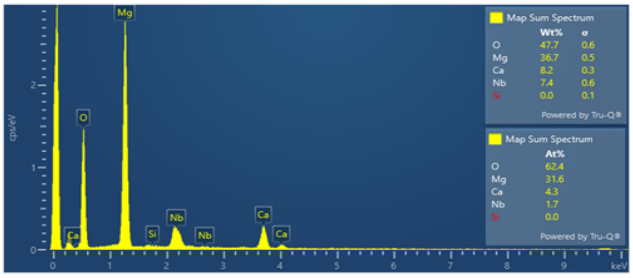

Fig. 5: EDX Map sum Spectra peaks of Niobium doped Calcium magnisium Silicate phosphor (Milled).

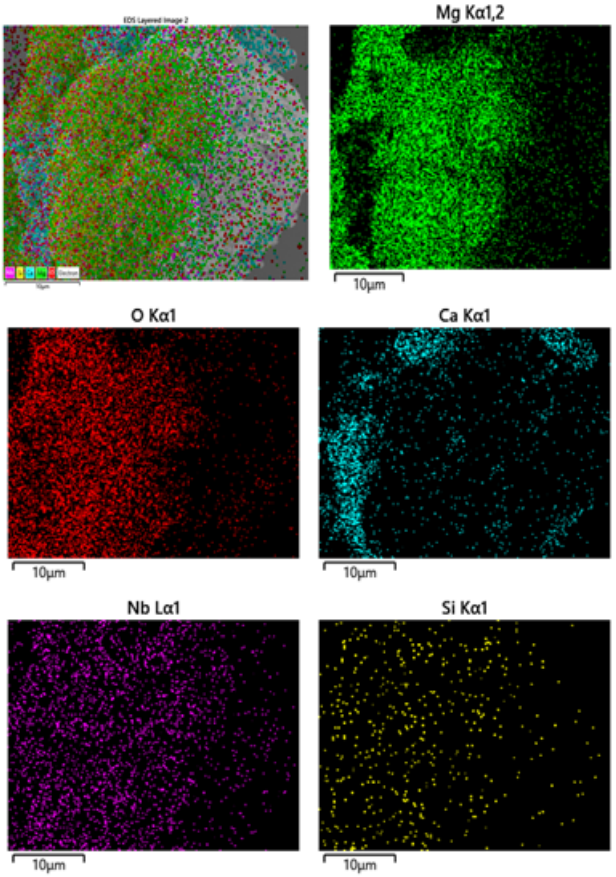

Fig.6: EDX Maping of Niobium doped Calcium magnisium Silicate phosphor (Map sum Specrum).

3.4. Fourier transforms infrared Spectroscopy (FTIR)

The Fourier Transform Infra-Red Spectroscopy (FTIR) spectrum has been widely used for the identification of

organic and inorganic compounds. The FTIR spectrum has been shown in (Fig. 7 A) grass extracted silicate (TEOS Substitute) and (Fig. 7 B) CMS: 1.0% Nb^{5+} phosphor. The FTIR spectra were recorded in the range of (4000 cm^{-1} to 400 cm^{-1}) to obtain the figure print results.

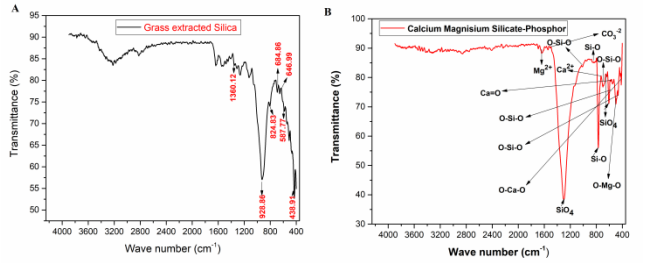

Fig.7: FTIR Spectra: A. (Green synthesized TEOS Substitute-Bulk), B. 1.0% Nb^{5+} doped Calcium Magnesium Silicate phosphor- -milled.

At 928.82 cm^{-1} allocated a result of (Si-O-Si) asymmetric stretch, 824.83 cm^{-1} (Si-O) symmetric stretch, 587.77 cm^{-1} and 438.91 cm^{-1} (Si-O-Si) vibration mode and 1360.12cm^{-1}, 68 6.81cm^{-1} and 646.91 cm^{-1} allocated to existence of SiO_4 group (see Fig. 7A). (Fig.7 B) show Calcium Magnesium Silicate phosphor;- At 842.92 cm^{-1} allocated to Si-O symmetric stretch, 586.52 and 482.82 cm^{-1} were Si-O-Si vibrational mode, 1300.61 cm^{-1} SiO_4 group existence, 415.80 cm^{-1} O-Ca-O bending modes, 490.49 cm^{-1} O-Mg-O bending mode, 1024.89 cm^{-1} symmetric stretching of Si-O-Si , 1641.10 cm^{-1} Mg^{+2} vibrational bond, 1500 cm^{-1} big vibration of carbonate and 737.90 cm^{-1} Ca^{+2} bending peak. As concentrations of dopant vary from 0.2% to 1.0% the intensity became highly enhanced and slightly shifted to new position. This might be due to the shift in the wave number position following the variation in the dopant concentration. The FTIR spectrum of calcium magnesium silicate powders calcined at 500 ˚C in **(Fig.7 B)** is in a good agreement with what is reported in literature [14]. **(Fig.7 A)** Grass extracts FTIR spectra at bulk confirms the presence of TEOS substitute silica groups.

3.5. UV-Visible Spectroscopy (UV-Vis)

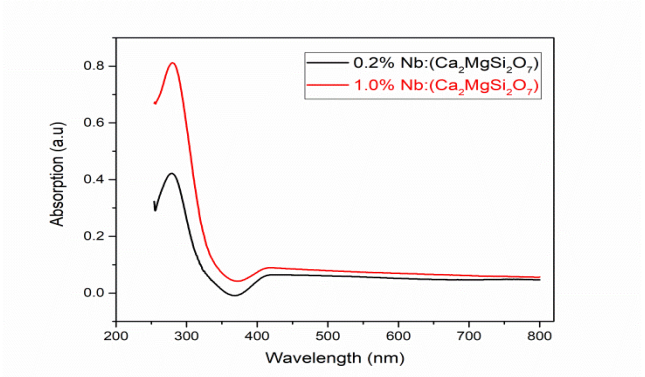

Fig. 8: Shows UV-Vis absorption spectra of 0.2% and 1.0% Nb^{5+}: doped Calcium Magnesium Silicate phosphor.

Typical UV-Vis spectra of $Ca_2MgSi_2O_7$:xNb^{5+} phosphor was shown by Fig.8. The result showed also the peak absorption occurs at wavelength of 280nm for 1.0% and at wavelength of 278nm for 0.2% that were excited at wavelength of 280 nm. From the results we observed that Nb^{5+} doping has significant effects on the peaks intensity: when we vary the dopants concentration from 0.2% to 1.0% the intensity become doubled (See Fig. 8).

3.6. Photoluminescence (PL)

We examine the excitation and emission spectra of milled 0.2 % and 1.0 % Nb^{5+} doped $Ca_2MgSi_2O_7$ phosphor excited from 260nm-360nm wavelength ranges. We obtained visible emission from blue to red region at different wavelength having various intensity (121 to 834) a.u. **(See Fig. 9 (A, B).** The excitation at (280nm) spectrum of $Ca_2MgSi_2O_7$:xNb^{5+} phosphor monitored at 564 nm emission given in **Fig. 9 (B)** has maximum emission intensity of 866 (a.u.). The spectrum of $Ca_2MgSi_2O_7$:xNb^{5+} phosphor has also exhibited a broad band in the UV region centered at about 280 nm. For excitation at wavelength of (280nm), as we increase the concentration of Nb^{5+} from 0.2 % to 1.0 %, the emission intensity highly enhanced from (305 a.u. to 866 a.u.) **See Fig.9 B.** From the UV-Vis absorption and PL analysis, effects of the niobium ion dopant concentration were remains consistent in both analyses, since the previous results of Uv-vis i.e. as concentration of the dopant increases the intensity highly enhanced at the same wavelength of 280nm for both absorption and excitation of Uv-Vis and PL results at the respective wavelength.

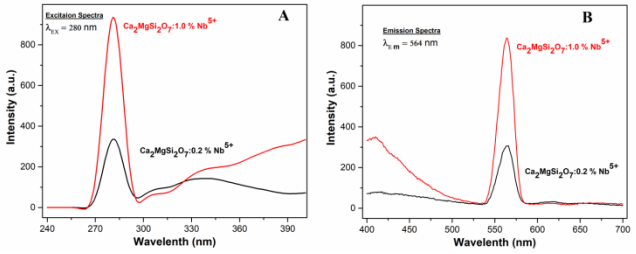

Fig. 9: Photoluminescence spectra of 0.2% Nb^{5+} and 1.0% Nb^{5+} doped Calcium Magnesium Silicate phosphor: (A = Excitation, B = Emission).

4 Conclusions

A novel luminescent phosphor of $Ca_2MgSi_2O_7$:xNb^{5+} was successfully synthesized via sol gel methods using *stenotaphrum secundatum* grass extract as TEOS substitute and its optical properties were investigated. XRD pattern showed tetragonal akermanite crystal structure. FTIR confirms the existence of functional groups in the phosphor and it has also demonstrated *stenotaphrum secundatum* grass extract is a good source of silica. SEM image indicated the surface morphology is rough and aggregated having porous structure. The EDX spectra confirmed the existence of present elements in $Ca_2MgSi_2O_7$:xNb^{5+}

phosphor. The EDX results also revealed that there were relatively uniform distributions of particles in the system. The excitation spectra indicated the phosphor can be effectively excited by ultraviolet (UV) light, making it attractive as conversion phosphor for LED applications. The $Ca_2MgSi_2O_7:Nb^{5+}$ phosphor exhibits bright emission excited at wavelength of 280 nm. Photoluminescence measurements showed that the phosphor exhibited emission peak with good intensity (866 a.u.) at wavelength of 564 nm, corresponding to nearly green emission, indicating that it has favorable properties for application as near ultraviolet LED conversion phosphor. The concentration of niobium ion showed a significant effect on the intensity of absorptions and photoluminescence.

Acknowledgement

We gratefully acknowledge departments of materials science and engineering and chemistry, Jimma University, for their XRD and FTIR facilities, respectively. For SEM, PL and UV-Vis facilities, we thank Adama Science and Technology University. Authors are also thankful to Dr. Negara Abdissa, Dr. Tokuma Negisho, and Physics Department for their great cooperation. We are also heartily grateful to College of Natural Sciences Post Graduate and Research Coordinating Office, Jimma University for the financial support.

References

[1] I.P. Sahu, D.P. Bisen, N. Brahme, L. Wanjari, R.K. Tamrakar, Structural characterization and luminescence properties of bluish-green-emitting SrCaMgSi2O7:Eu2+, Dy3+ phosphor by solid-state reaction method, Research on Chemical Intermediates., **41,** 8797-881(2015).

[2] E. Karacaoglu, B. Karasu, Effect of activators and calcination on luminescence properties of akermanite type phosphors, Indian Journal of Chemistry. Section A, **54**, 1394-1401 (2015).

[3] S. Sharma, S. Dubey, The significant properties of silicate based luminescent nanomaterials in various fields of applications: a review, International Journal of Scientific Research in Physics and Applied Sciences., **9**, 37-41(2021).

[4] F. Wang, H. Chen, Influence of Mn2+ doping on the emission spectrum of Sr2La8(SiO4)6O2:Eu(2+,3+) phosphor, Inorganic Chemistry Communications., **142** 109625(2022).

[5] N. Sboui, H. Agougui, M. Jabli, K. Boughzala, Synthesis, physico-chemical, and structural properties of silicate apatites: Effect of synthetic methods on apatite structure and dye removal, Inorganic Chemistry Communications., **142,**109628 (2022).

[6] T.G.V.M. Rao, A.R. Kumar, N. Veeraiah, M.R. Reddy, Optical and structural investigation of Sm3+–Nd3+ co-doped in magnesium lead borosilicate glasses, Journal of Physics and Chemistry of Solids., 74, 410-417 (2013).

[7] G.J. Talwar, C.P. Joshi, S.V. Moharil, S.M. Dhopte, P.L. Muthal, V.K. Kondawar, Combustion synthesis of Sr3MgSi2O8:Eu2+ and Sr2MgSi2O7:Eu2+ phosphors, Journal of Luminescence., **129**, 1239-1241(2009).

[8] I.P. Sahu, D.P. Bisen, N. Brahme, R.K. Tamrakar, Photoluminescence properties of europium doped di-strontium magnesium di-silicate phosphor by solid state reaction method, Journal of Radiation Research and Applied Sciences., **8**, 104-109(2015).

[9] P. Imchen, M. Ziekhrü, B.K. Zhimomi, T. Phucho, Biosynthesis of silver nanoparticles using the extract of Alpinia galanga rhizome and Rhus semialata fruit and their antibacterial activity, Inorganic Chemistry Communications., **142**, 109599(2022).

[10] Z. Gharari, P. Hanachi, T.R. Walker, Green synthesized Ag-nanoparticles using Scutellaria multicaulis stem extract and their selective cytotoxicity against breast cancer, Analytical Biochemistry., **653**, 114786(2022).

[11] D. Borah, P. Saikia, P. Sarmah, D. Gogoi, J. Rout, N.N. Ghosh, C.R. Bhattacharjee, Composition controllable alga-mediated green synthesis of covellite CuS nanostructure: An efficient photocatalyst for degradation of toxic dye, Inorganic Chemistry Communications., **142**, 109608 (2022).

[12] .S. Sharma, S.K. Dubey, A.K. Diwakar, S. Pandey, Novel White Light Emitting (Ca2MgSi2O7:Dy3+) Phosphor. , Journal of Materials Science Research and Reviews., **8**, 164-171(2021).

[13] JOINT COMMITTEE ON POWDER DIFFRACTION STANDARDS, Analytical Chemistry., **42**,81A-81A (1970).

[14] R. Choudhary, S. Koppala, S. Swamiappan, Bioactivity studies of calcium magnesium silicate prepared from eggshell waste by sol–gel combustion synthesis, Journal of Asian Ceramic Societies., **3**, 173-177(2015).